

Electronic Supplementary Information for

**Implications of Cation-Disordered Grain Boundary on the
Electrochemical Performance of $\text{LiNi}_{0.5}\text{Co}_{0.2}\text{Mn}_{0.3}\text{O}_2$
Cathode Material for Lithium Ion Batteries**

Jae-Hyun Shim^{ab}, Jong-San Im^c, Hyosik Kang^d, Namchul Cho^e, Young-Min Kim^{*af}, and
Sanghun Lee^{*d}

^a*Department of Energy Science, Sungkyunkwan University (SKKU), Suwon 16419, Republic of Korea.*

^b*Department of Advanced Materials and Energy Engineering, Dongshin University, Naju 58245, Republic of Korea.*

^c*Battery R&D Center, Samsung SDI Co. Ltd., Suwon 16678, Republic of Korea.*

^d*Department of Nanochemistry, Gachon University, Seongnam 13120, Republic of Korea.*

^e*Department of Energy System, Soonchunhyang University, Asan 31538, Republic of Korea.*

^f*Center for Integrated Nanostructure Physics, Institute for Basic Science (IBS), Suwon 16419, Republic of Korea.*

*Corresponding author.

E-mail address: youngmk@skku.edu (Y.-M. Kim), sanghunlee@gachon.ac.kr (S. Lee)

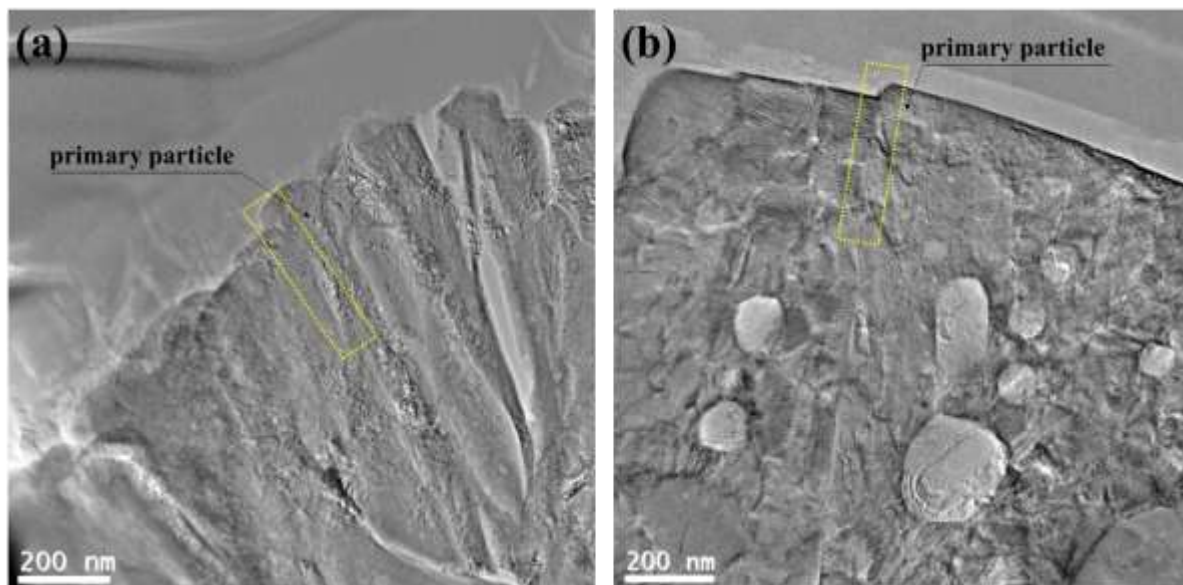


Figure S1. Low-magnification bright-field TEM images of (a) LiTM101 and (b) LiTM107, respectively. The yellow dotted rectangles in the images show the representative regions of interest across grain boundary that were analyzed via our atom-resolved STEM-EDX/EELS techniques.

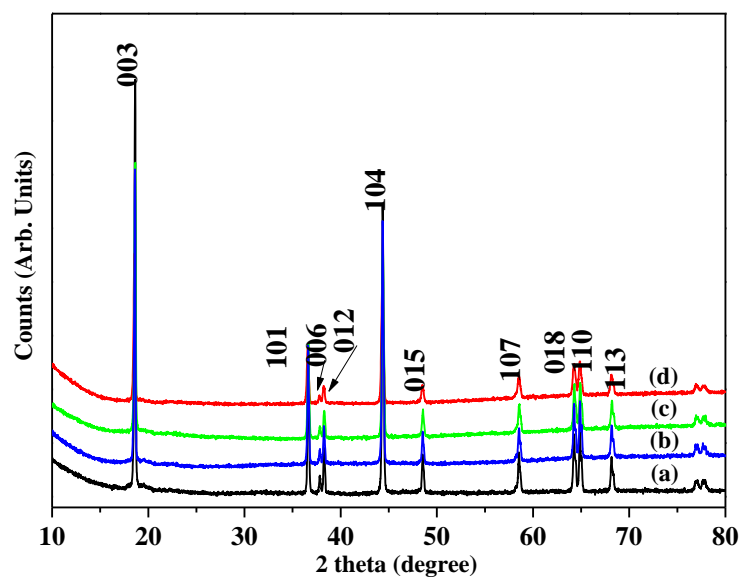


Figure S2. XRD patterns of $\text{LiNi}_{0.5}\text{Co}_{0.2}\text{Mn}_{0.3}\text{O}_2$ samples with different Li contents: (a) LiTM101, (b) LiTM103, (c) LiTM105, and (d) LiTM107.

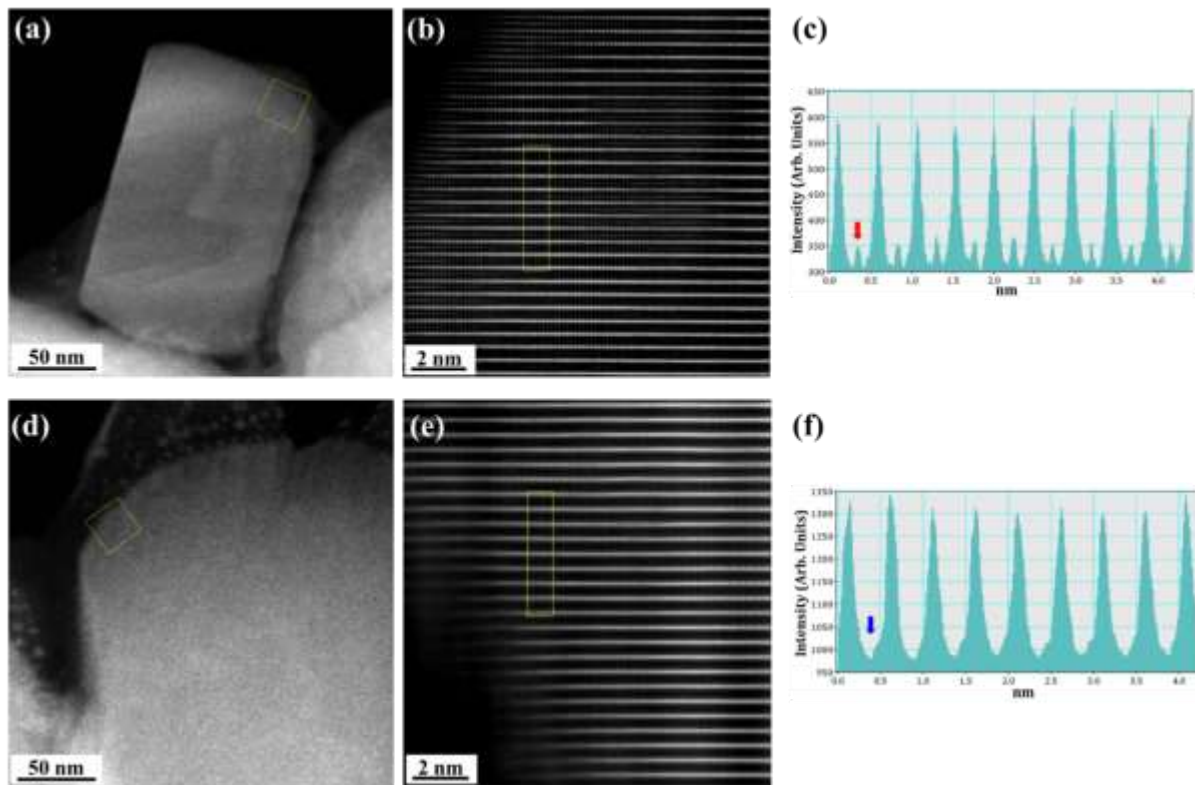


Figure S3. STEM observation on the surfaces of the two samples, LiTM101 and LiTM107. (a,d) Low-magnification images and (b,e) atom-resolved images (for the yellow boxed area) of LiTM101 and LiTM107, respectively. (c,f) Intensity profiles obtained along the vertical rectangular marked in the HAADF STEM images of the two samples. Note that cation disorder phenomenon at the surface is only observed in LiTM101 sample (see red arrow) as observed at grain boundaries of the sample.

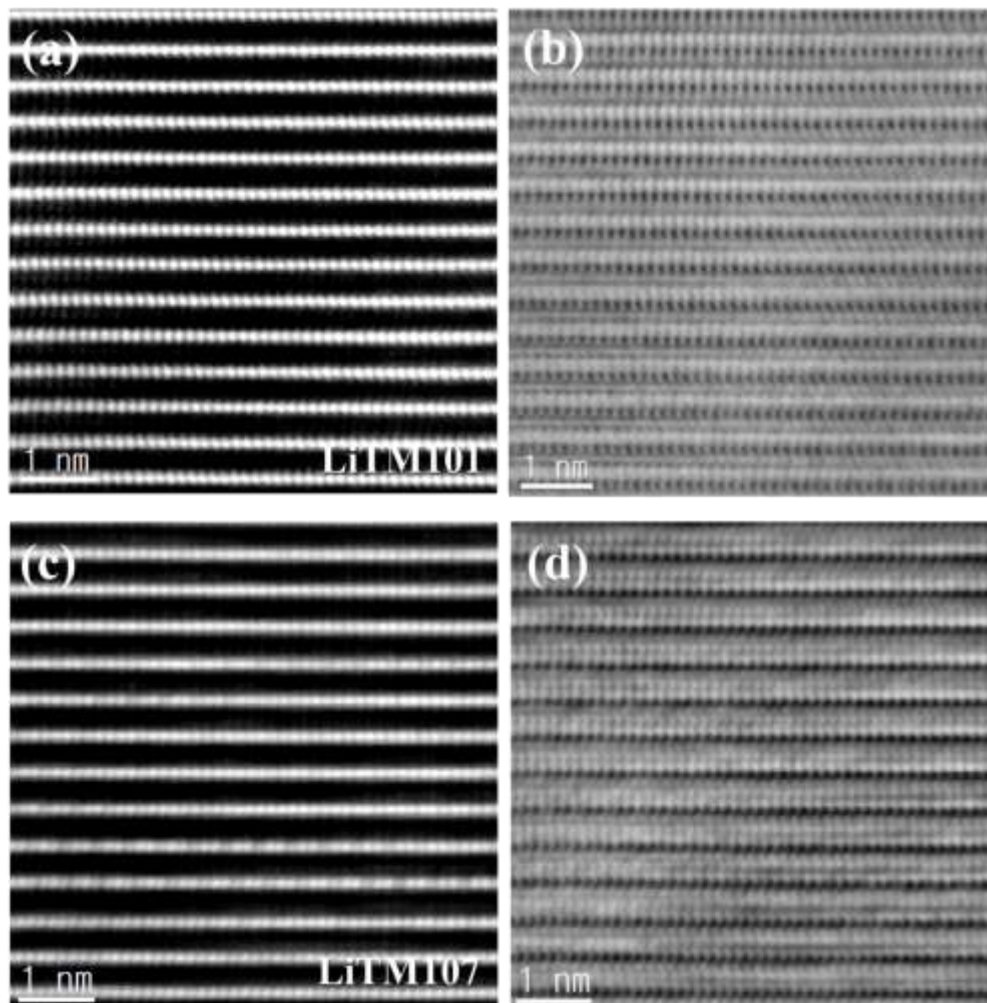


Figure S4. Atomic-structures of the bulk parts deep inside the secondary particles of LiTM101 and LiTM107, respectively. (a,c) HAADF-STEM images and (b,d) the simultaneously acquired ABF-STEM images of the two samples, LiTM101 and LiTM107, respectively.

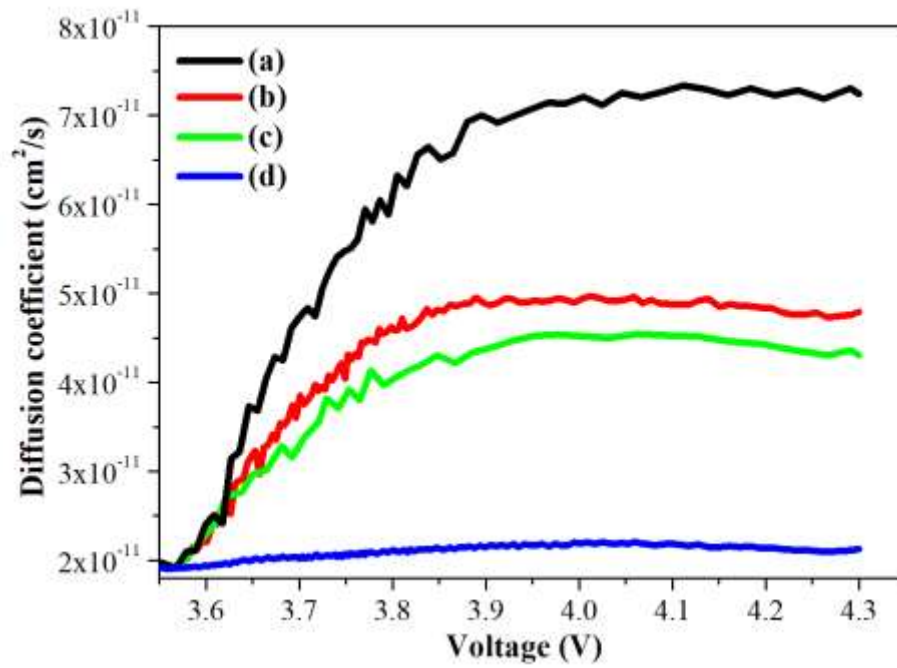


Figure S5. Lithium diffusion coefficients of (a) LiTM101, (b) LiTM103, (c) LiTM105, and (d) LiTM107 electrodes calculated from GITT curves as a function of the applied cell voltage.

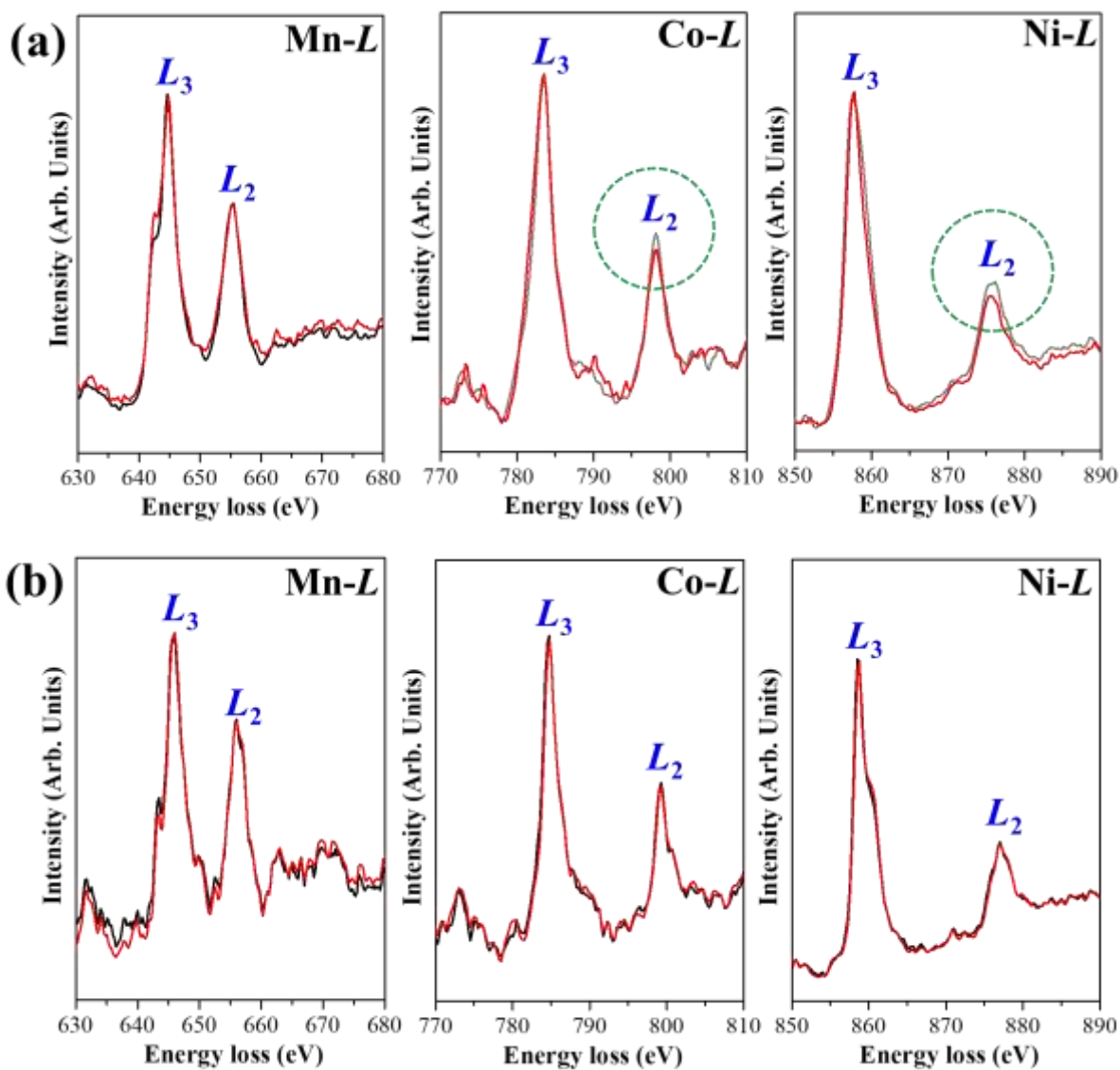


Figure S6. Comparison of $L_{2,3}$ edges of transition metals, Mn, Co, and Ni between bulk (black) and grain boundary (red) regions of (a) LiTM101 and (b) LiTM107, respectively.

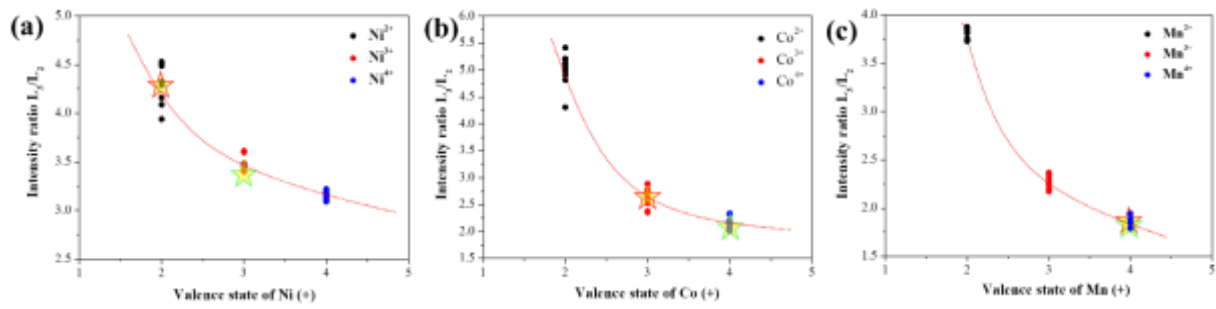


Figure S7. Empirical fitting curves of (a) Ni, (b) Co, and (c) Mn valence states as a function of Ni, Co, and Mn L_3/L_2 EELS intensity ratios with reference to the known standard samples. NiO, LiNiO₂, and NiO₂ were used as standard samples for Ni valences of 2+, 3+, and 4+, respectively. NiO₂ was prepared by an electrochemical lithium extraction using a nonaqueous lithium cell charged up to 5V. Likewise, for measuring Co valence states of 2+, 3+, and 4+, CoO, LiCoO₂, and CoO₂ were used as standards and for Mn valence states, MnO, Mn₂O₃, and MnO₂ were the standard samples, respectively. For the LiTM101 sample exhibiting cation disorder behavior, the measured valence states of each transition metal in the grain boundary and bulk region are marked as green and red pentagrams, respectively, which confirms that our estimation of valence states for the LiTM samples is reliable because all EELS experiments were performed under the same acquisition condition.